Inorganic Chemistry

Article

pubs.acs.org/IC

Nature of Si−H Interactions in a Series of Ruthenium Silazane Complexes Using Multinuclear Solid-State NMR and Neutron Diffraction

Katharine A. Smart,[†,‡] Mary Grellier,*[,†,‡] Yannick Coppel,[†,‡] Laure Vendier,[†,‡] Sax A. Mason,[§] Silvia C. Capelli,[§] Alberto Albinati,[∥] Virginia Montiel-Palma,[⊥] Miguel A. Muñoz-Hernández,[⊥] and Sylviane Sabo-Etienne*[,†,‡]

[†]LCC (Laboratoire de Chimie de Coordination), CNRS, 205 Route de Narbonne, F-31077 Toulouse, France

[‡]Université de Toulouse, UPS, INPT, F-31077 Toulouse, France

[§]Institut Laue−Langevin, 6 rue Jules Horowitz, BP 156, 38042 Grenoble Cedex 9, France

[∥]Dipartimento di Chimica, Università di Milano, Via C. Golgi, 19, 20133 Milan, Italy

[⊥]Centro de Investigaciones Químicas, Universidad Autónoma del Estado de Morelos, Avenida Universidad 1001, Cuernavaca, Morelos, C. P. 62209, México

Supporting Information

ABSTRACT: Three new N-heterocyclic-silazane compounds, **1a−c**, were prepared and employed as bidentate ligands to ruthenium, resulting in a series of [Ru(H){(κ-*Si,N*-($SiMe_2$-N-heterocycle)}$_3$] complexes (**3a−c**) featuring the same $RuSi_3H$ motif. Detailed structural characterization of the $RuSi_3H$ complexes with X-ray diffraction, and in the case of triazabicyclo complex [Ru(H){κ-Si,N-($SiMe_2$)($C_7H_{12}N_3$)}$_3$] (**3a**), neutron diffraction, enabled a reliable description of the molecular geometry. The hydride ligand of (**3a**) is located closer to two of the silicon atoms than it is to the third. Such a geometry differs from that of the previously reported complex [Ru(H){(κ-*Si,N*-($SiMe_2$)N($SiMe_2$H)(C_5H_4N)}$_3$] (**3d**), also characterized by neutron diffraction, where the hydride was found to be equidistant from all three silicon atoms. A DFT study revealed that the symmetric and less regular isomers are essentially degenerate. Information on the dynamics and on the Ru···H···Si interactions was gained from multinuclear solid-state (^{1}H wPMLG, ^{29}Si CP MAS, and 2D ^{1}H−^{29}Si dipolar HETCOR experiments) and solution NMR studies. The corresponding intermediate complexes, [Ru{κ-Si,N-($SiMe_2$-N-heterocycle)}(η^4-C_8H_{12})(η^3-C_8H_{11})] (**2a−c**), involving a single silazane ligand were isolated and characterized by multinuclear NMR and X-ray diffraction. Protonation of the $RuSi_3H$ complexes was also studied. Reaction of **3a** with NH_4PF_6 gave rise to [Ru(H)(η^2-H −$SiMe_2$)κ-N-($C_7H_{12}N_3$){κ-Si,N-($SiMe_2$)($C_7H_{12}N_3$)}$_2$]$^+$[PF_6]$^-$ (**4aPF$_6$**) which was isolated and characterized by NMR spectroscopy, X-ray crystallography, and DFT studies. The nature of the Si−H interactions in this silazane series was analyzed in detail.

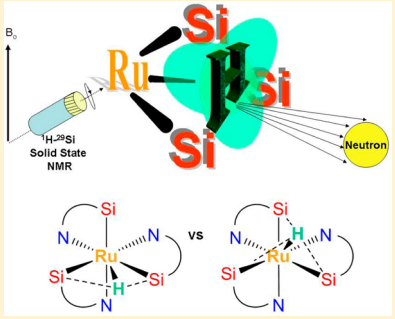

INTRODUCTION

The description of nonclassical interactions in (H−E)−metal (E = Si, B, H, C, etc.) complexes has received careful attention over several decades.[1] Classically Si−H bonds undergo oxidative addition (OA) with transition-metal fragments, but many nonclassical (H−Si)−metal complexes have been identified as different arrested states along the OA coordinate. The existence of σ-(H−Si)ML_n species, with significant bonding interaction between Si and H, is widely accepted on the basis of experimental and theoretical studies. For weaker M−Si−H interactions, ambiguity arises over whether residual bonding remains or complete OA has occurred. Geometric parameters, particularly Si−H separation, are often used when assessing the extent of M−H−Si interactions. For example, we consider Si−H distances of 1.6−1.9 Å as indicative of η^2-(H−Si) coordination to ruthenium.[2] Various nonclassical systems have been proposed to account for relatively long (>1.9 Å) H−Si separations where spectroscopic and theoretical studies suggest interaction of the silicon and hydrogen atoms. These systems, including interligand hypervalent interactions (IHI),[3] asymmetric oxidation addition products (ASOAP),[4] and secondary interactions between silicon and hydrogen atoms (SISHA),[2,5] were established for complexes involving different metals and ligand sets, and it is difficult to formulate an overarching description.

To draw meaningful comparisons between related species, we have developed a series of complexes bearing the same $RuSi_3H$ motif incorporating different N-heterocyclic-silane bidentate ligands. Si−N bonds link the N-heterocyclic and silane components, placing the ligands in the silazane compound class, a group with diverse applications: from

Received: October 29, 2013
Published: January 6, 2014

   dx.doi.org/10.1021/ic4027199 | *Inorg. Chem.* 2014, 53, 1156−1165

protecting-group reagents to monomers in the preparation of polysilazanes.[6] Silazanes with additional Si−H functionality, hydridosilazanes, have the potential for multicenter reactivity, although there has been little development of such chemistry in areas other than ceramics. However, a few reports featuring silazane moieties have recently been published. For example, the ruthenium-catalyzed dehydrogenative coupling of N-heterocycles with secondary and tertiary silanes to form Si−N bonds was described by Oestreich and co-workers as an alternative to nucleophilic substitution of a chlorosilane by an amine.[7] Additionally, Anwander and co-workers highlight an expedient use of hydridosilazanes as spectroscopic probes for the characterization of iron silylamide-grafted mesoporous silica.[8]

Our initial entry into the study of silazanes was the reaction of the ruthenium dihydride (bis)dihydrogen complex $[RuH_2(\eta^2\text{-}H_2)_2(PCy_3)_2]$ with $HN(SiMe_2H)_2$ and the isolation of $[RuH_2\{(\eta^2\text{-}HSiMe_2)_2NH\}(PCy_3)_2]$, a complex featuring nonclassical coordination of two Si−H bonds. We were able to demonstrate the selective ruthenium-catalyzed deuteration of the Si−H bonds of $HN(SiMe_2H)_2$ under an atmosphere of D_2.[9] The resulting deutero silazane, $HN(SiMe_2D)_2$, was subsequently employed for a solid-state deuterium (^2H) NMR study of the molecular dynamics of $-SiMe_2D$ grafted to the surface of silica.[10] We continued in the field of silazanes with the coordination of pyridyl-functionalized silazanes by ruthenium. Notably, the incorporation of three silazane ligands and a single hydride was possible using $[Ru(\eta^4\text{-}C_8H_{12})(\eta^6\text{-}C_8H_{10})]$ as a precursor, giving rise to the complexes $[Ru(H)\{(\kappa\text{-}Si,N\text{-}(SiMe_2)N(SiMe_2H)(C_5H_4N)\}_3]$ **3d**[11] and $[Ru(H)\{(\kappa\text{-}Si,N\text{-}(SiMe_2)N(Me)(C_5H_4N)\}_3]$ **3e**.[12] Complex **3d** was found by X-ray and neutron diffraction to have three Si−H distances equal by symmetry (2.154(8) Å neutron), whereas the hydride of **3e** was found by X-ray diffraction to be in a less symmetric environment, with two Si−H distances shorter than the third (1.97(3), 2.00(3), and 2.33(3) Å). We now report the synthesis of three N-heterocyclic-silazane compounds bearing rigid or flexible bicyclic N-heterocycles with varying electronic properties for comparison with the originally reported ruthenium silazane complexes **3d** and **3e**. A range of techniques, including multinuclear solid-state and solution NMR spectroscopy, X-ray and neutron diffraction, and DFT calculations, were employed for the detailed characterization of the reported compounds. In particular, the difficulty in characterizing secondary interactions and assigning metal oxidation states in highly fluxional systems was circumvented because of the combination of $^1H-^{29}Si$ solid-state and solution NMR experiments, as now demonstrated for **3d** and new triazabicyclo complex $[Ru(H)\{\kappa\text{-}Si,N\text{-}(SiMe_2)\text{-}(C_7H_{12}N_3)\}_3]$ (**3a**).

RESULTS AND DISCUSSION

Synthesis of Compounds 1a−1c. N-Heterocyclic-(dimethyl)silazane compounds **1a−1c**, displayed in Chart 1, were prepared by deprotonation of the corresponding N-heterocycle with an appropriate base followed by nucleophilic substitution of chloride from chlorodimethylsilane according to a standard method.[13] An equiv of *n*-butyllithium was used to deprotonate 7-azaindole. However, it was necessary to use an equiv of KH in the preparation of **1a** and **1c** because of unwanted side reactions of *n*-BuLi with 1,5,7-triazabicyclo[4.4.0]dec-5-ene in the synthesis of **1a** and 6-chloro-7-deazapurine in that of **1c**. After work up, the pure compounds were obtained as colorless oils. Characteristic NMR

Chart 1. N-Heterocyclic(dimethyl)silazane Compounds 1a−1e

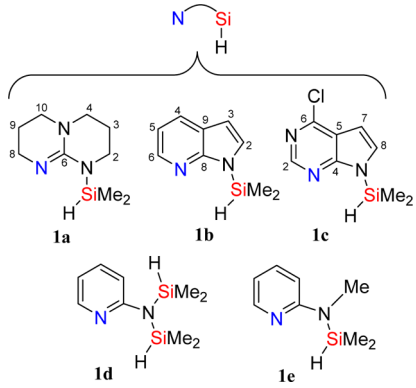

signals were observed: high-field ^{29}Si chemical shifts of δ −11.4 (**1a**), δ 3.84 (**1b**), and δ 1.32 (**1c**) together with septets in the ^1H spectra for the Si−H protons at δ 4.95 (**1a**), δ 5.26 (**1b**), and δ 4.98 (**1c**). The values are presented in Table 1.

Table 1. Selected ^1H and ^{29}Si Solution NMR Parameters of 1a−1c, 3a−3c, and 4a

	δ_{Si}	$\delta_{Si-H}/\delta_{Hydride}$	J_{SiH}
1a	−11.44	4.95	191
1b	−3.84	5.26	209
1c	−1.32	4.98	214
3a	57.4	−15.83	9
3b	58.6	−13.97	9
3c	61.3	−14.62	9
4a	45.7	−16.81	17

Synthesis of Complexes 3a−3c. Addition of the N-heterocyclic(dimethyl)silazanes, **1a−1c**, to pentane solutions of $[Ru(\eta^4\text{-}C_8H_{12})(\eta^6\text{-}C_8H_{10})]$ led to the formation of corresponding complexes **2a−2c** by oxidative addition of the Si−H bond. **2a−2c** involve two alkenyl ligands together with the N-heterocyclic(dimethyl)silazane (Scheme 1). The complexes

Scheme 1. Synthesis of Complexes 2 and 3

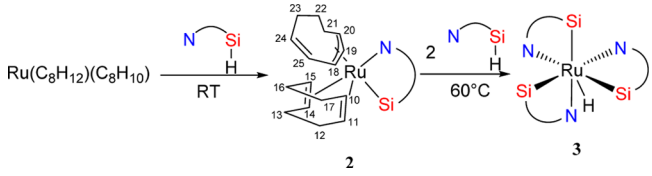

were characterized by multinuclear NMR and X-ray diffraction (Supporting Information) and display properties similar to the previously reported complex $[Ru\{\kappa\text{-}Si,N\text{-}(SiMe_2)N(Me)\text{-}(C_5H_4N)\}(\eta^4\text{-}C_8H_{12})(\eta^3\text{-}C_8H_{11})]$.[12]

Reaction of **2a−2c** with a slight excess of 2 equiv of the corresponding ligand (**1a−1c**) at 60 °C gave rise to complexes **3a−3c**, which accommodate three silyl moieties together with a hydride ligand at ruthenium. The ^1H NMR spectra of **3a−3c** feature signals corresponding to three $SiMe_2$ groups in comparison to a single hydride ligand. Coupling between the hydride and silyl groups, J_{SiHapp} = 9 Hz, is inferred from the ^{29}Si satellites observed for the high-field hydride singlets, resonating close to δ −15. Although 9 Hz is a low silicon hydrogen coupling constant, it does represent a non-negligible interaction

dx.doi.org/10.1021/ic4027199 | Inorg. Chem. 2014, 53, 1156−1165

between the two elements.[1e] Single silicon resonances are observed in the $^{29}Si\{^{1}H\}$ NMR of **3a** at δ 57.40, **3b** at δ 58.55, and **3c** at δ 61.32, indicating that the $SiMe_2$ groups are equivalent in solution. At 193 K, no change is observed for **3a**, and a single ^{29}Si signal is detected in solution ($^{29}Si,^{1}H$)-HSQC NMR spectroscopy (see the next section for solid-state NMR data). The silicon NMR chemical shifts and silicon-hydride coupling constants of ligands **1a**, **1b**, and **1c** are interesting to compare with those of the corresponding complexes. The difference in silicon NMR chemical shifts ($\Delta\delta_{Si}$) is 10.12 ppm for **1a**−**1c**, 4.80 ppm for **2a**−**2c**, and 3.92 for **3a**−**3c**. Together with the significant change in the value of the ^{29}Si chemical shifts of the ligands once coordinated to ruthenium, there is also a decrease in the difference of the chemical shifts, suggesting that the varying electronic influences of the N-heterocyclic groups are modulated by the presence of the metal. Additionally, ΔJ_{SiH} = 22.4 for the ligands, but there is no difference in the silicon-hydride coupling constants for complexes **3a**−**3c**.

Discussion of the H Atom Position: Comparison of X-ray, Neutron, and DFT data. The coordination of three N-heterocyclic ligands together with the hydride in **3a**−**3c** was confirmed by X-ray crystallography. In the case of **3a**, we were also able to obtain a structure by neutron diffraction (Figure 1).

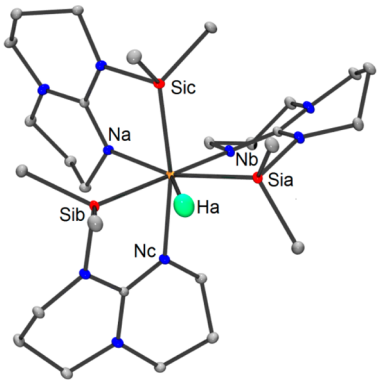

Figure 1. Neutron structure of **3a** (50% probability ellipsoids). Hydrogen atoms other than H_a are omitted for clarity.

Neutron diffraction permits the accurate and precise location of hydrogen atoms, whereas systematic errors lead to underestimated E−H distances derived from X-ray diffraction.[1b] Given that the classification of Si−H bond type is often highly reliant on Si−H distance, it is valuable to obtain neutron diffraction data and to make comparisons with data from X-ray and DFT. Geometric parameters of **3a** and **3c** obtained by neutron diffraction (**3a**), X-ray crystallography, and DFT are given in Table 2. A more detailed analysis of the DFT parameters will be presented in the following section.

Complexes **3a**−**3c** feature the same motif, three N-heterocyclic-silazane ligands and a hydride ligand, as the previously reported $[Ru(H)\{\kappa\text{-Si,N-}(SiMe_2)N(C_5H_4N)\text{-}(SiMe_2H)\}_3]$ (**3d**) and $[Ru(H)\{\kappa\text{-Si,N-}(SiMe_2)N(Me)\text{-}(C_5H_4N)\}_3]$ (**3e**) complexes. A neutron diffraction study of **3d** indicated a symmetric structure, with the hydride positioned equidistant, 2.154(8) Å, from the three silicon atoms.[11] In contrast, complex **3e** was found to be less symmetric by X-ray crystallography with two Si−H distances, 1.97(3) and 2.00(3) Å, that are shorter than the third, 2.33(3) Å.[12] Complexes **3a**−**3c** enable further investigation of the general phenomenon of the position of a hydrogen atom in the presence of three silicon atoms. The Si−H bond distances of **3a**, determined by neutron diffraction, are notably different, 1.874(3), 2.099(3), and 3.032(3) Å, and the hydride is considerably closer to two of the silicon atoms than it is to the third, similar to complex **3e**. However, in **3a**, the Si−H distance of 1.874(3) Å is within the range normally given for σ-complex formulation, where a distance below 1.9 Å is indicative of a nonclassical three-center-two-electron bond. At distances between 1.9 and 2.4 Å, there is evidence from experimental and theoretical studies for secondary interactions between silicon and hydrogen atoms (SISHA), and the Si−H separation of 2.098(3) Å is well within this range. The longer Si···H separation, 3.037(3) Å, is above the limit and is too long for any interaction.[2] As one would expect, the neutron H−Ru−Si angles (H_a−Ru−Si_a, 53.5(1)°; H_a−Ru−Si_b, 61.8(1)°; and H_a−Ru−Si_c, 100.8(1)°) become more obtuse as the separation between the silicon and hydrogen atom increases.

Comparing the X-ray, neutron, and DFT data of **3a**, one notes that the Ru−H and Si−H X-ray distances are less accurate and precise than those of neutron diffraction. However, the X-ray distances are still in agreement at the 3σ level (given the large ESD) with the neutron diffraction values and consistent with the DFT Ru−H and Si−H distances (isomer **3a**^{a}, see the next section). We also note the very good agreement between neutron values and those calculated by DFT. The X-ray, neutron, and DFT data we collected for **3d**

Table 2. Geometrical Parameters of 3a and 3c Determined by X-ray and Neutron Diffraction and DFT Calculations[a]

	3a		3a[a]	3c	3c[a]	3c[s]
	X-ray	neutron	DFT	X-ray	DFT	DFT
Ru−H_a	1.56(2)	1.599(3)	1.590	1.59(9)	1.588	1.562
Si_a−H_a	1.81(2)	1.874(3)	1.879	1.83(10)	1.916	2.158
Si_b−H_a	2.14(2)	2.099(3)	2.100	2.09(10)	2.028	2.164
Si_c−H_a	2.98(2)	3.032(3)	3.057	2.77(9)	2.915	2.176
Ru−Si_a	2.3123(4)	2.314(2)	2.343	2.3543(2)	2.391	2.367
Ru−Si_b	2.3116(4)	2.313(2)	2.343	2.3681(2)	2.389	2.368
Ru−Si_c	2.2959(4)	2.294(2)	2.323	2.3280(2)	2.359	2.368
N_a−Ru−Si_a	159.63(3)	159.63(6)	159.7	166.35(2)	165.2	169.3
N_b−Ru−Si_b	168.48(3)	168.32(5)	168.9	166.40(2)	167.4	169.3
N_c−Ru−Si_c	168.63(4)	168.58(6)	169.6	172.61(2)	173.6	169.4

[a] **3a**^{a}−**c**^{a} are the isomers with the hydrogen atom that is positioned closer to two silicon atoms than it is to the third (Figure 4, **3**^{a}). **3c**^{s} is the symmetric isomers with three equal Si−H distances (Figure 4, **3**^{s}).

dx.doi.org/10.1021/ic4027199 | Inorg. Chem. 2014, 53, 1156−1165

feature the same trend: for the neutron structure, the Ru−H bond length is 1.559(7) Å, for the X-ray, 1.41(5) Å, and for DFT, 1.557 Å.[11] The same is true for the Si−H separation: neutron, 2.154(8) Å; X-ray, 2.120(9) Å; and DFT, 2.162 Å (**3d**^{s}). Thus, it seems that a reliable description of the $RuSi_3H$ moiety may be obtained by complementary use of X-ray and DFT methods once validated by neutron diffraction data.

Furthermore, the positions of the ruthenium, silicon, and nitrogen atoms are representative of overall structural geometry, as these atoms are accurately located by X-ray diffraction. As an illustration for **3a**, the Ru−Si distances are influenced by the nature of the corresponding Si−H interactions. The shortest Ru−Si separation, 2.295(2) Å (neutron), 2.2959(4) Å (X-ray), is found for the silicon atom furthest from the hydride ligand, as would be expected for a ruthenium-silyl moiety rather than a nonclassical Ru−H−Si system. The corresponding Si−Ru−N angles are also indicative of the Si−H interaction: more obtuse angles are observed when the implicated silicon is located further from the hydride.

The crystal structure of **3c** is similar to those of **3a** and **3e**, with two Si−H distances shorter than the third. The Si−H separations (Å) are 1.83(10), X-ray and 1.916, DFT; 2.09(10), X-ray and 2.028, DFT; and 2.77(9), X-ray and 2.915, DFT. The shortest Si−H distance of **3c** is borderline between η^2-complex and SISHA formulation. For **3c**, we cautiously identify a SISHA interaction rather than a η^2-complex on the basis of DFT values superior to 1.9 Å. Again, the positions of the heavy atoms are indicative of the overall molecular geometry. The shortest Ru−Si distance, Ru−Si_c 2.3280(2) Å, is found for the silicon atom furthest from the hydrogen atom, Si_c−H_a 2.77(9) Å. Moreover, the angle N_c−Ru−Si_c, 172.61(2)°, is more obtuse than the other two N−Ru−Si angles of 166.35(2)° and 166.40(2)°.

Complex **3b** is an interesting case, presenting two different structures depicted in Figure 2: crystals are trigonal when

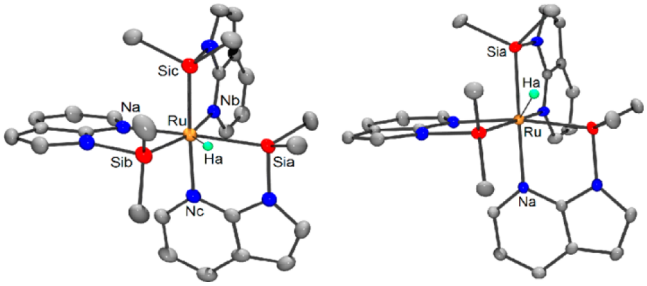

Figure 2. X-ray molecular structures of **3b hex** (left) and **3b pent** (right) (50% probability ellipsoids with hydrogen atoms represented by green spheres or excluded for clarity).

obtained from pentane but triclinic when grown from hexane. X-ray and DFT geometric parameters are displayed in Table 3. For the crystal of **3b** grown in pentane, the symmetry of the structure dictates three equal Si−H distances of 2.116(5) Å. The hexane crystal has two Si−H distances (Å), 1.91(3) and 1.92(3), shorter than the third, 2.72(3). Once more, the N−Ru−Si angles are valuable tools for describing molecular geometry. The angle is again more obtuse for the silicon atom located furthest from hydrogen: N_c−Ru−Si_c is 174.24(6)° compared with 167.94(6)° and 166.05(6)° for N_a−Ru−Si_a and N_b−Ru−Si_b, respectively. There is evidently very little difference in energy between species with two relatively strong SISHA silicon hydrogen interactions and three slightly weaker Si−H interactions, with a minor change in the crystallization

Table 3. Geometrical Parameters of 3b Determined by X-ray Diffraction of a Crystal Grown in Pentane (3b pent) or Hexane (3b hex) and DFT Calculations

	3b pent	3b^{s}	3b hex	3b^{a}
	X-ray	DFT	X-ray	DFT
Ru−H_a	1.58(2)	1.562	1.42(3)	1.588
Si_a−H_a	2.116(5)	2.158	1.91(3)	2.027
Si_b−H_a		2.164	1.92(3)	1.919
Si_c−H_a		2.176	2.72(3)	2.913
Ru−Si_a	2.3370(6)	2.367	2.3575(9)	2.383
Ru−Si_b		2.368	2.3505(9)	2.384
Ru−Si_c		2.368	2.3206(8)	2.354
N_a−Ru−Si_a		169.3	167.94(6)	166.9
N_b−Ru−Si_b		169.3	166.05(6)	165.3
N_c−Ru−Si_c	170.27(3)	169.4	174.24(6)	173.4

solvent being sufficient to favor one form over the other in **3b**. The DFT energy calculations are presented in the next section.

Optimized DFT/B3PW91 Structures 3a^{a}−e^{a} and 3b^{s}−e^{s} and Associated Transition States. The DFT-calculated nonsimplified structures of **3a**−**3e** adopt different isomeric forms associated with very flat potential-energy surfaces (Figure 3). **3a^{a}**−**e^{a}** are isomers with the hydrogen atom positioned closer to two silicon atoms than the third (Figure 4, **3^{a}**). **3b^{s}**−**e^{s}** are symmetric isomers with three equal Si−H distances (Figure 4, **3^{s}**). DFT optimization of **3a^{a}**−**e^{a}** and **3b^{s}**−**e^{s}** led to minima in the potential-energy surface (no imaginary frequency) for each compound. As displayed in Figure 3, the difference in energy between the optimized structures (**3x^{a}** vs **3x^{s}** with **x** = **b**−**e**) is extremely small (0.06−1.92 kJ mol^{-1}). The structures with H_a located between two silicon atoms are marginally more stable for **3a^{a}**−**c^{a}** and **3e^{a}**. The isomer corresponding to H_a equidistant from three silicon atoms is only the most stable for **3d^{s}**. The transition-state **TS3x^{a}x^{s}** (with **x** = **b**−**e**) involved in the conversion between isomer **3x^{a}** and **3x^{s}** has a geometry and an energy close to the less stable isomer. Complex **3a^{a}** is optimized as a minimum, but the species featuring the H_a atom equidistant from three silicon atoms corresponds to a transition state (**TS3a**) involved in the exchange between H_a and two of the three coordinated silicon atoms rather than another minimum. It is possible that the 1,5,7-triazabicyclo[4.4.0]dec-6-ene ligand of **3a** has different steric demands to the aromatic species employed in **3d**, **3e**, **3b**, and **3c**, and a symmetric structure for **3a** is consequently rendered unfavorable.

Protonation of 3a Leading to 4aPF$_6$ or 4aBAr$^{F}_4$ and Deprotonation of 4aPF$_6$. The reaction of **3a** with the acidic compounds NH_4PF_6 or $[H(OEt_2)_2]^+[\{3,5\text{-}(CF_3)_2C_6H_3\}_4B]^-$ ($\{3,5\text{-}(CF_3)_2C_6H_3\}_4B$ = BAr^{F}_4) gave rise to protonated species **4aPF$_6$** and **4aBAr$^{F}_4$**, respectively (Scheme 2). The integrated ^{1}H NMR spectrum indicates that there are two hydride ligands in relation to three $SiMe_2$ groups. For **4aPF$_6$**, the hydride signal at δ −15.71 has ^{29}Si satellites (J_{SiHapp} = 17 Hz), and no decoalesence of the signal was observed at 193 K. The J_{SiHapp} of **4a** is markedly larger than the value for **3a** (J_{SiHapp} = 9 Hz), suggesting stronger Si−H interactions. Additionally, one signal is observed in the (^{29}Si,^{1}Hi)-HSQC NMR spectrum at δ 45.7 at 298 K and also at 193 K, reflecting the fluxionality of these species in solution.

The presence of two hydrides and three $SiMe_2$ groups was confirmed by X-ray diffraction on the yellow crystals of **4aPF$_6$** and of **4aBAr$^{F}_4$**. Geometrical parameters are presented in Table 4. **4aPF$_6$** and **4aBAr$^{F}_4$** are similar to the previously reported

dx.doi.org/10.1021/ic4027199 | Inorg. Chem. 2014, 53, 1156−1165

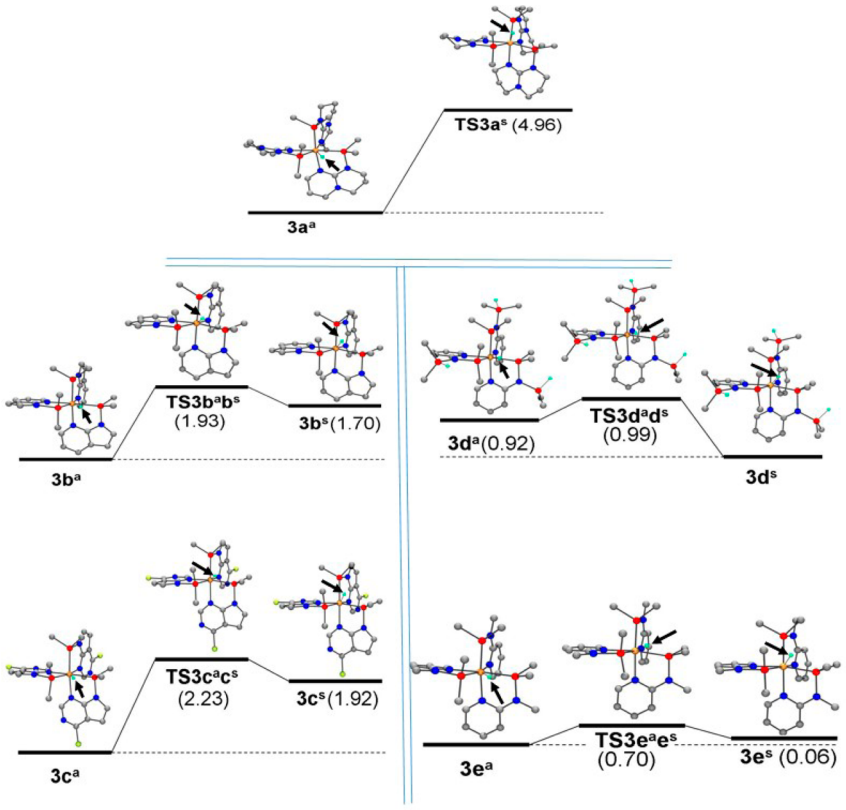

Figure 3. Optimized structures $\mathbf{3a^a}$– $\mathbf{e^a}$ and $\mathbf{3b^s}$–$\mathbf{e^s}$ and associated transition-states **TS3a** and $\mathbf{TS3x^ax^s}$ with **x** = **b**–**e**. The colors of the atoms are Ru, orange; N, blue; Si, red; H, green (hydride location indicated by a black arrow), and C, gray. Energies are given in in kilojoules per mole.

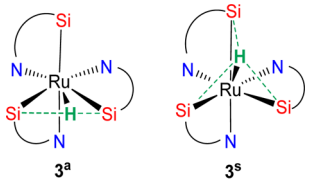

Figure 4. Isomers of **3**. $\mathbf{3^a}$ is the isomer with the hydrogen atom positioned closer to two silicon atoms than the third. $\mathbf{3^s}$ is the symmetric isomer with three equal Si–H distances.

Scheme 2. Reversible Deprotonation of 3a Leading to 4a

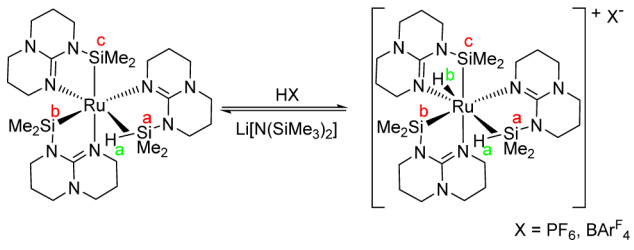

complex $[Ru(\eta^2\text{–H-SiMe}_2)N(Me)\kappa\text{-N-}(C_5H_4N)\{\kappa\text{-Si,N-}(SiMe_2)N(Me)(C_5H_4N)\}]^+BAr^F$ ($\mathbf{4eBAr^F_4}$).[12] The three complexes have been formulated with one η^2-Si–H interaction and two SISHA. For **4**, the DFT distances are (Å) Si_a–H_a, 1.756; Si_b–H_b, 1.977; and Si_c–H_c, 1.980. For $\mathbf{4eBAr^F_4}$, the Si–H distances (Å) were determined by neutron diffraction and are similar to those of **4**: Si_a–H_a, 1.74(1); Si_b–H_b, 1.95(1); and Si_c–H_c, 2.00(1). The same trends in Ru–Si and N–Ru–Si parameters are observed for **4**: the shortest Si–H separation correlates with the longest Ru–Si and the most acute Si–Ru–N. The X-ray data of $\mathbf{4aPF_6}$ and $\mathbf{4aBAr^F_4}$ are remarkably consistent, suggesting that reliable comparison of structural features involving hydrides may be obtained from X-ray diffraction data when good sets of data are available.

Table 4. Geometrical Parameters of 4a Determined by X-ray Diffraction and DFT Calculations

	$\mathbf{4aPF_6}$	$\mathbf{4aBAr^F_4}$	$\mathbf{4a^+}$
	X-ray	X-ray	DFT
$Ru–H_a$	1.52(3)	1.51(3)	1.597
$Ru–H_b$	1.54(3)	1.50(4)	1.582
$Si_a–H_a$	1.71(3)	1.70(3)	1.756
$Si_b–H_a$	2.34(3)	2.28(3)	2.295
$Si_c–H_a$	3.22(3)	3.22(4)	3.324
$Si_a–H_b$	3.03(3)	3.02(3)	3.098
$Si_b–H_b$	1.96(3)	1.92(4)	1.977
$Si_c–H_b$	1.95(3)	2.00(4)	1.980
$Ru–Si_a$	2.4146(6)	2.4143(7)	2.440
$Ru–Si_b$	2.3813(6)	2.3802(7)	2.409
$Ru–Si_c$	2.3932(6)	2.3824(7)	2.406
$Si_a–Ru–N_a$	159.88(5)	160.67(6)	160.1
$Si_b–Ru–N_b$	162.61(5)	163.23(6)	163.1
$Si_c–Ru–N_c$	168.83(5)	167.64(6)	168.9

There was no protonation when $[H(OEt_2)_2]^+[\{3,5\text{-}(CF_3)_2C_6H_3\}_4B]^-$ reacted with **3b** and **3c**, reflecting the reduced basicity of these complexes with respect to complex **3a**. It was possible to deprotonate cleanly $\mathbf{4aPF_6}$ and generate **3a** by reaction with an equiv of $Li[N(SiMe_3)_2]$ in THF.

Discussion of the H Atom Position: Solid-State versus Solution NMR Spectroscopy. The $RuSi_3H$ complexes **3**

dx.doi.org/10.1021/ic4027199 | Inorg. Chem. 2014, 53, 1156–1165

display a single $^{29}Si\{^{1}H\}$ NMR signal in solution, and it is thus impossible to identify the presence of any preferential and/or significant interaction between the hydride and at least one of the Si atoms. With all of the structural data in hand, particularly the neutron structures for complexes **3a** and **3d**, we draw additional information from solid-state NMR. The use of this technique remains rather limited in organometallic chemistry.[14] Solid-state NMR is a very useful tool in surface chemistry, particularly in the case of silica materials, but very few data can be found for silane transition-metal systems.[1b,14a] Recently, we used $^{1}H-^{31}P$ CP/MAS NMR experiments to understand an equilibrium phenomenon in an agostic phosphinoborane complex.[15] We have now implemented ^{1}H wPMLG, ^{29}Si CP MAS, and 2D $^{1}H-^{29}Si$ dipolar HETCOR experiments (see the Experimental Section) to detect hydride and silicon atoms and, most noteworthy, any interaction between them. The neutron structure obtained for complex **3d** showed a highly symmetrical geometry, with the three Si−H distances (2.154(8) Å) being equal by the imposed crystallographic symmetry. It should be noted that although the geometries from diffraction may be the results of symmetry-averaged geometrical parameters, solid-state NMR data will reflect the local geometry of a single molecule that may be lower than the crystallographic one. In solution, the $^{29}Si\{^{1}H\}$ NMR signal for the metal-bound Si appeared at δ 64.94, whereas the dangling Si atoms resonated at δ −14.24. In the solid state, the same behavior is observed, and the corresponding correlations are shown in Figure 5. Thus, **3d**

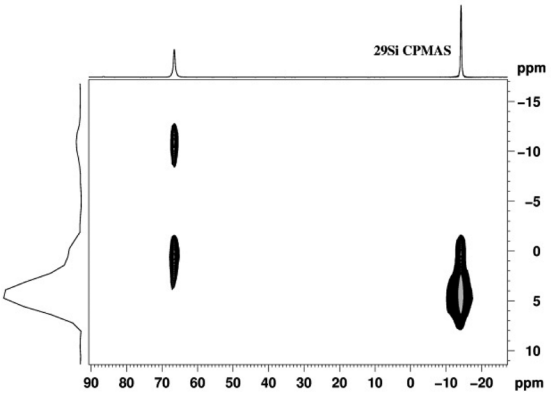

Figure 5. Two-dimensional $^{1}H-^{29}Si$ dipolar HETCOR spectrum (contact time 100 μs) for complex $Ru(H)\{(\kappa\text{-}Si,N\text{-}(SiMe_2)N\text{-}(SiMe_2H)(C_5H_4N)\}_3]$ (**3d**) in the solid state.

is really a highly symmetrical system both in solution and in the solid state (Table 5). The case of complex **3a** is strikingly different. The neutron structure reveals a less symmetric geometry, with the hydride considerably closer to two of the silicon atoms than it is to the third: 1.874(3), 2.099(3), and 3.032(3) Å. In solution at 298 K, the $^{29}Si\{^{1}H\}$ NMR signal for

Table 5. ^{29}Si Solid-State NMR Chemical Shifts and Neutron Diffraction Si−H Distances (Å) Corresponding to 3a and 3d

	$\delta_{Si\ solid}$	Si−H
3a	56.6	1.874(3)
	50.8	2.099(3)
	62.4	3.032(3)
3d	66.1	2.154(8)
	−14.6	1.481(5)

the three Si atoms appears at δ 57.4, and a single resonance is again observed at 193 K. In the solid state, three distinct ^{29}Si signals are apparent in the CP MAS experiment at δ 50.8, δ 56.6, and δ 62.4. Most revealingly, from the 2D $^{1}H-^{29}Si$ dipolar HETCOR experiment depicted in Figure 6, the central signal at

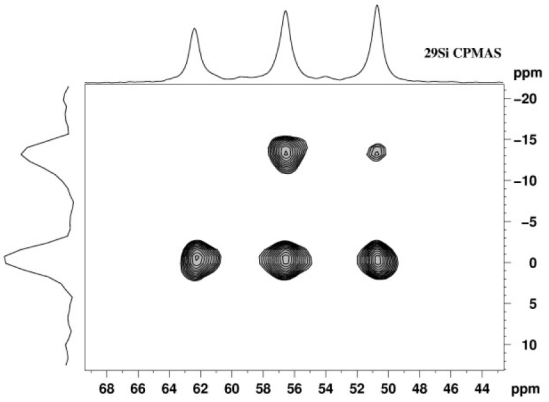

Figure 6. Two-dimensional $^{1}H-^{29}Si$ dipolar HETCOR spectrum (contact time 200 μs) for complex $[Ru(H)\{\kappa\text{-}Si,N\text{-}(SiMe_2)\text{-}(C_7H_{12}N_3)\}_3]$ (**3a**) in the solid state.

δ 56.6 displays a strong correlation peak with the hydride signal at δ −15 and the signal at δ 50.8, a correlation of lower intensity, whereas the third signal at δ 62.4 presents no correlation with the hydride and only with the methyl groups. The correlations are observed with contact time from 100 to 1000 μs (see the Supporting Information). Such a scenario is in line with the neutron data, and the proposal of the hydride being involved in a η^2-(H−Si) interaction (δ 56.6, 1.874(3) Å), a SISHA interaction (δ 50.8, 2.099(3) Å), and no interaction with the third Si atom ((δ 62.4, 3.032(3) Å). Such a situation would formally correspond to a ruthenium(II) complex.

CONCLUSIONS

We have designed three new N-heterocyclic-silazane ligands, and their coordination to a ruthenium center has given rise to two series of complexes. The incorporation of a single ligand leads to species of the type $[Ru\{\kappa\text{-}Si,N\text{-}(SiMe_2\text{-}N\text{-heterocycle})\}(\eta^4\text{-}C_8H_{12})(\eta^3\text{-}C_8H_{11})]$, **2**. The olefinic ligands of **2** are readily displaced on reaction with further equivalents of the N-heterocyclic-silazane, yielding $[Ru(H)\{(\kappa\text{-}Si,N\text{-}(SiMe_2)\text{-}(N\text{-heterocycle})\}_3]$ species, $RuSi_3H$, **3**.

Crystal structures of the $RuSi_3H$ complexes were obtained as two structural isomers with the hydride located closer to two of the three silicon atoms or with the hydride being equidistant from all three because of the imposed crystallographic symmetry. A combination of X-ray, neutron, and DFT data enabled us to describe accurately the geometry of the $RuSi_3H$ compounds and to assess the reliability of employing X-ray and DFT parameters alone when neutron diffraction is unfeasible. It is noteworthy that the neutron diffraction study of **3a** adds to the relatively scarce neutron data on M−H−Si systems.[4b,11,12,16] The data are strikingly different from those previously obtained for **3d**.[11] In **3d**, the structure is symmetric with three equal Si−H separations (2.154(8) Å), and the hydride coincides with the C_3 axis. The complex was thus formulated as a hydridotrisilyl ruthenium(IV) complex stabilized by SISHA interactions. This formulation is now confirmed by the new solid-state NMR data. In contrast, in **3a**, a less regular structure is obtained, with the hydride

dx.doi.org/10.1021/ic4027199 | Inorg. Chem. 2014, 53, 1156−1165

considerably closer to two of the three silicon atoms. Moreover, the Si−H distance of 1.874(3) Å is within the range given for σ complexes, and **3a** could thus be formulated as a ruthenium(II) complex stabilized by one SISHA interaction (2.099(3) Å). In solution, the $^{29}Si\{^{1}H\}$ NMR spectra of all the $RuSi_3H$ species feature a single resonance for equivalent silicon environments, even at low temperature, indicating the highly dynamic nature of the molecules. However, in the solid state, the 2D $^{1}H-^{29}Si$ dipolar HETCOR spectrum clearly identifies three different Si environments for **3a**, and the extent of their interaction with the neighbor hydride can be qualitatively evidenced: a η^2-(H−Si) interaction (δ 56, 1.874(3) Å), a SISHA interaction (δ 50, 2.099(3) Å), and no interaction with the third Si atom ((δ 62, 3.032(3) Å). It becomes increasingly clear that the organometallic community could benefit from the use of solid-state NMR techniques in a more routine way. When dealing with hydrogen atoms difficult to locate by X-ray diffraction and with the inherent constraints associated with neutron measurements, the use of well-selected solid-state NMR sequences can provide telling information on the interaction involving a hydrogen atom with its neighbors.

Finally, the theoretical study resulted in essentially degenerate structures for the symmetric and less symmetric isomers. The potential-energy surfaces are relatively featureless, and there is a very low barrier for passing from the Si_3H interaction to that of Si_2H. It is clear that varying the N-heterocyclic ligand has little effect on the predominance of one isomer over another, particularly in solution. However, the ligands do have an impact on the basicity of the complexes: **3a** was readily protonated in contrast to **3b** and **3c**. Studies of the electrochemistry of the $RuSi_3H$ complexes will continue to probe the influence of the electronic properties of the ligands on the ruthenium center and will be reported in due course.

EXPERIMENTAL SECTION

General Methods. Manipulations were carried out following standard Schlenk line and glovebox techniques with O_2 < 1 ppm and Ar as the inert gas. Solvents were dried using a MBraun SPS system column. Deuterated solvents were freeze−pump−thaw degassed and stored under Ar and over 4 Å molecular sieves. THF-d_8 was dried over sodium. Ru(η^4-C_8H_{12})(η^6-C_8H_{10}) was prepared according to a previously published literature method.[17] Unless otherwise indicated, commercially available reagents were used as supplied, and for the most part were purchased from Aldrich or Alfa Aesar. Solution NMR spectra were collected on several machines: a Bruker 500 MHz Avance, a Bruker 400 MHz Avance, a Bruker 300 MHz Avance, and a Bruker 300 MHz DPX. Solid-state NMR experiments were recorded on a Bruker Avance 400 spectrometer equipped with a 4 mm probe operating at 399.60 MHz for ^{1}H and 79.39 MHz for ^{29}Si. Samples were loaded into 4 mm ZrO_2 rotors under argon in a glovebox. All experiments were done with a MAS frequency of 8 kHz and at room temperature. All chemical shifts for ^{1}H and ^{29}Si are relative to TMS. ^{1}H with wPMLG3 (windowed phase-modulated Lee−Goldburg)[18] homonuclear decoupling were carried out at an effective field of 80 kHz and an acquisition window of 8 μs. ^{29}Si-CP/MAS spectra were recorded with a recycle delay of 5 s and a contact time of 3 ms. Two-dimensional $^{1}H-^{29}Si$ dipolar HETCOR were performed with FSLG (frequency-switched Lee−Goldburg),[19] decoupling at an effective field of 80 kHz during ^{1}H evolution period followed by polarization transfer from ^{1}H to ^{29}Si with contact time from 100 to 1000 μs. Chemical shifts are given in units of ppm, and coupling constants, Hz. Mass spectroscopy was carried out using a TSQ 7000 Thermo Electron mass spectrometer. Infrared spectroscopy was carried out using a PerkinElmer 1725 spectrometer for Nujol mulls pressed between KBr disks. Microanalyses were performed at the Laboratoire de Chimie de Coordination on a PerkinElmer 2400 series II analyzer.

*Synthesis of 1,5,7-Triazabicyclo[4.4.0]dec-6-ene-N-dimethylsilazane (**1a**).* 1,5,7-Triazabicyclo[4.4.0]dec-5-ene (2.000 g, 14.37 mmol) was dissolved in THF (50 mL), and KH (0.580 g, 14.37 mmol) was added slowly to the stirring solution to form a white suspension in a colorless solution. After stirring for 12 h, the mixture was cooled to −6 °C, and $HSiMe_2Cl$ (1.600 mL, 14.37 mmol) in THF (5 mL) was added dropwise. The pale pink solution was allowed to warm to room temperature and stirred for 2 h. The solvent was removed under reduced pressure to leave a yellow residue. The product was extracted with pentane (40 mL), giving rise to a pink solution. The pentane was removed under reduced pressure, and the resulting pink oil was purified by trap-to-trap distillation to yield a colorless oil (1.74 g, 61%). ^{1}H NMR (400.13 MHz, C_6D_6, 298 K): (see **1a** in Chart 1 for atom numeration) 4.95 (sept, 1H, Si−H, $^{3}J_{HH}$ = 2.8, $^{1}J_{SiH}$ = 191.3), 3.30 (t, 4H, H2 and H8 $C_7H_{12}N_3$, $^{3}J_{HH}$ = 5.6), 2.67 (t, 4H, H4 and H10 $C_7H_{12}N_3$, $^{3}J_{HH}$ = 6.0), 1.58 (dt, 4H, H3 and H9 $C_7H_{12}N_3$, $^{3}J_{HH}$ = 6.0, $^{3}J_{HH}$ = 4.4), 0.70 (d, 6H, $SiMe_2$, $^{3}J_{HH}$ = 3.2, $^{2}J_{SiH}$ = 10.4). $^{13}C\{^{1}H\}$ NMR (100.62 MHz, C_6D_6, 298 K): 150.77 (s, C6 $C_7H_{12}N_3$), 47.83 (s, C4 and C10 $C_7H_{12}N_3$), 43.00 (s, C2 and C8 $C_7H_{12}N_3$), 23.89 (s, C3 and C9 $C_7H_{12}N_3$), −0.01 ($SiMe_2$). ^{29}Si $\{^{1}H\}$ DEPT NMR (79.50 MHz, C_6D_6, 298 K) −11.44. Positive CI-MS: m/z 140 ($C_7H_{12}N_3$ + 2) (100%). IR (Nujol mull, cm^{-1}) 2143 (strong), 2088 (medium) (ν_{Si-H}). The two bands are accounted for by different conformers according to DFT optimization of the molecule.

*Synthesis of (7-Azaindole)dimethylsilazane (**1b**).* 7-Azaindole (5.000 g, 42.32 mmol) was dissolved in Et_2O (90 mL) and cooled to 0 °C before *n*-BuLi (26.45 mL, 1.6 M in hexane, 42.32 mmol) was added dropwise. After 1 h of stirring, an Et_2O solution (15 mL) of $HSiMe_2Cl$ (4.603 mL, 42.32 mmol) was added to the pale yellow suspension, leading to the formation of a white precipitate. A pale yellow solution was obtained after filtration through Celite, and the solvent was evaporated. The resulting yellow oil was purified by trap-to-trap distillation at 80 °C to afford a colorless oil (6.5 g, 86%). ^{1}H NMR (400.13 MHz, C_6D_6, 298 K): (see **1b** in Chart 1 for atom numeration) 8.49 (dd, 1H, H6 $C_7H_5N_2$, $^{3}J_{HH}$ = 4.7, $^{4}J_{HH}$ = 1.5), 7.75 (dd, 1H, H4 $C_7H_5N_2$, $^{3}J_{HH}$ = 7.8, $^{4}J_{HH}$ = 1.6), 7.10 (d, 1H, H2 $C_7H_5N_2$, $^{3}J_{HH}$ = 3.4), 6.92 (dd, 1H, H5 $C_7H_5N_2$, $^{3}J_{HH}$ = 7.8, $^{3}J_{HH}$ = 4.7), 6.53 (d, 1H, H3 $C_7H_5N_2$, $^{3}J_{HH}$ = 3.5), 5.26 (sept, 1H, SiH, $^{3}J_{HH}$ = 3.3, $^{1}J_{SiH}$ = 209.1), 0.54 (d, 6H, $SiMe_2$, $^{2}J_{SiH}$ = 10.4, $^{3}J_{HH}$ = 3.3). $^{13}C\{^{1}H\}$ NMR (100.61 MHz, C_6D_6, 298 K): 154.05 (s, C8 $C_7H_5N_2$), 142.97 (s, C6 $C_7H_5N_2$), 130.27 (s, C2 $C_7H_5N_2$), 128.10 (s, C4 $C_7H_5N_2$), 122.93 (s, C9 $C_7H_5N_2$), 116.36 (s, C5 $C_7H_5N_2$), 103.43 (s, C3 $C_7H_5N_2$), −2.84 ($SiMe_2$). ^{29}Si $\{^{1}H\}$ DEPT NMR (79.50 MHz, C_6D_6, 298 K): −3.84 (s). Positive CI MS m/z = 177.1 [M + 1] 13%, 119 [$C_7H_5N_2$ + 2] 100%. IR (Nujol mull, cm^{-1}) 2150 (medium) (ν_{Si-H}).

*Synthesis of 6-Chloro-7-deazapurine-N-dimethylsilazane (**1c**).* 6-Chloro-7-deazapurine (0.700 g, 4.56 mmol) was dissolved in THF (30 mL), and KH (0.180 g, 4.56 mmol) was added slowly to the stirring solution, liberating a gas and forming a yellow solution. After stirring for 2 h, the mixture was cooled to −20 °C, and $HSiMe_2Cl$ (0.506 mL, 4.56 mmol) in THF (5 mL) was added dropwise. The resulting cloudy yellow solution was allowed to warm to room temperature and stirred for 2 h. The solvent was removed under reduced pressure to leave a yellow residue. The product was extracted with pentane (40 mL), giving rise to a pale yellow solution. The pentane was removed under reduced pressure, and the resulting yellow oil was purified by trap-to-trap distillation to yield a colorless oil (0.60 g, 62%). ^{1}H NMR (400.13 MHz, C_6D_6, 298 K): (see **1c** in Chart 1 for atom numeration) 8.77 (s, 1H, H2 $C_6H_3N_3Cl$), 6.72 (d, 1H, H8 $C_6H_3N_3Cl$, $^{3}J_{HH}$ = 3.5), 6.52 (d, 1H, H7 $C_6H_3N_3Cl$, $^{3}J_{HH}$ = 3.5), 4.98 (sept, 1H, Si−H, $^{3}J_{HH}$ = 3.4, $^{1}J_{HSi}$ = 213.7), 0.35 (d, 6H, $SiMe_2$, $^{3}J_{HH}$ = 3.4, $^{2}J_{HSi}$ = 7.2). $^{13}C\{^{1}H\}$ NMR (100.61 MHz, C_6D_6, 298 K): 157.09 (s, C6 $C_6H_3N_3Cl$), 152.23 (s, C4 $C_6H_3N_3Cl$), 150.87 (s, C2 $C_6H_3N_3Cl$), 130.89 (s, C8 $C_6H_3N_3Cl$), 120.15 (s, C5 $C_6H_3N_3Cl$), 102.15 (s, C7 $C_6H_3N_3Cl$), −3.33 ($SiMe_2$). ^{29}Si $\{^{1}H\}$ DEPT NMR (79.50 MHz, C_6D_6, 298 K): −1.32. Positive CI-MS: m/z = 154 ($C_6H_3N_3Cl$ + 2) (100%).

*Synthesis of [Ru{κ-Si,N-($SiMe_2$)($C_7H_{12}N_3$)}(η^4-C_8H_{12})((η^3-C_8H_{11})] (**2a**).* A pentane solution (1 mL) of 1,5,7-triazabicyclo[4.4.0]dec-6-ene-*N*-dimethylsilazane (0.274 g, 1.43 mmol) was added to a pentane

dx.doi.org/10.1021/ic4027199 | Inorg. Chem. 2014, 53, 1156−1165

Table 6. Selected X-ray Data Collection and Refinement Parameters for 3a, 3b pent, 3b hex, 3c, 4aPF$_6$, and 4aBAr$^F_4$

	3a	3b pent	3b hex	3c	4aPF$_6$	4aBAr$^F_4$
formula	$C_{27}H_{55}N_9RuSi_3$	$C_{27}H_{34}N_6RuSi_3$	$C_{27}H_{34}N_6RuSi_3$, C_6H_{14}	$C_{24}H_{28}Cl_3N_9RuSi_3$	$C_{27}H_{55}N_9RuSi_3$, F_6P	$C_{27}H_{56}N_9RuSi_3$, $C_{32}H_{12}BF_{24}$
M_w	691.14	627.94	671.03	734.24	837.12	1555.37
cryst syst	monoclinic	trigonal	triclinic	monoclinic	triclinic	triclinic
space group	$P12_1/c1$	$R\bar{3}$	$P\bar{1}$	$P12_1/n1$	$P\bar{1}$	$P\bar{1}$
a (Å)	9.3827(2)	15.1399(9)	9.4948(13)	9.7355(6)	12.1134(2)	12.5626(3)
b (Å)	18.4666(5)	15.1399(9)	9.6324(13)	9.5108(6)	12.8423(3)	14.8823(4)
c (Å)	18.9153(5)	11.2499(17)	18.339(2)	33.6476(17)	16.9086(3)	18.5097(4)
α (deg)	90	90	95.782(2)	90	101.722(2)	90.5970(10)
β (deg)	92.5160(10)	90	98.830(2)	90.921(7)	105.697(2)	102.0120(10)
γ (deg)	90	120	105.106(2)	90	110.022(2)	93.5310(10)
V (Å^3)	3274.23(14)	2233.2(4)	1582.6(3)	3115.1(3)	2248.41(8)	3377.42(14)
Z	4	3	2	4	2	2
no. rflns collctd	32 217	36 511	5578	19 076	46 466	55 497
no. indep rflns	6685	4348	5063	4735	9166	13 633
no. params	371	115	372	371	438	889
R_1/wR_2, $I \geq 2\sigma(I)$	0.0199/0.0489	0.0173/0.0419	0.0336/0.0804	0.0496/0.1122	0.0310/0.0846	0.0333/0.0794

solution (6 mL) of [Ru(η^4-C_8H_{12})(η^6-C_8H_{10})] (0.300 g, 0.951 mmol) at room temperature. The formation of an orange precipitate was observed after 10 min. The solution was stirred for 15 h, and the precipitate was isolated by filtration and washed with pentane (2 × 3 mL) at −20 °C to afford the pure product, an orange powder (0.376 g, 78.0%). Crystals suitable for X-ray diffraction were grown from a pentane solution at room temperature. ^{1}H NMR (500.33 MHz, C_6D_6, 301 K): (see **2** in Chart 1 for atom numeration) 6.78 (dd, 1H, H25 C_8H_{11}, $^3J_{HH}$ = 10.9, $^3J_{HH}$ = 1.9), 5.49 (m, 1H, H24 C_8H_{11}), 5.47 (m, 1H, H18 C_8H_{11}), 3.80 (t, 1H, H19 C_8H_{11}, $^3J_{HH}$ = 8.7), 3.44 (m, 1H, H7 $C_7H_{12}N_3$), 3.44 (m, 1H, H15 C_8H_{12}), 3.38 (m, 1H, H16 C_8H_{12}), 3.31 (m, 1H, H23 C_8H_{11}), 3.15 (m, 1H, H4 or H5 $C_7H_{12}N_3$), 3.06 (m, 1H, H7 $C_7H_{12}N_3$), 3.02 (m, 1H, H3 or H6 $C_7H_{12}N_3$), 3.00 (m, 1H, H16 C_8H_{12}), 2.87 (sept, 1H, H4 or H5 $C_7H_{12}N_3$, $^3J_{HH}$ = 4.2), 2.73 (m, 1H, H20 C_8H_{11}), 2.67 (m, 1H, H14 C_8H_{12}), 2.67 (m, 1H, H4 or H5 $C_7H_{12}N_3$), 2.55 (dd, 1H, H3 or H6 $C_7H_{12}N_3$, $^3J_{HH}$ = 14.1, $^3J_{HH}$ = 8.8), 2.46 (m, 2H, H4 or H5 and H3 or H6, $C_7H_{12}N_3$), 2.42 (m, 1H, H2 $C_7H_{12}N_3$), 2.39 (m, 1H, C_8H_{12}), 2.39 (m, 1H, H2 $C_7H_{12}N_3$), 2.34 (m, 1H, C_8H_{11}), 2.34 (m, 2H, C_8H_{12}), 1.82 (m, 1H, H3 or H6 $C_7H_{12}N_3$, $^2J_{HH}$ = 18.0, $^3J_{HH}$ = 13.4, $^3J_{HH}$ = 8.9, $^3J_{HH}$ = 4.3), 1.61 (m, 1H, H22 C_8H_{11}), 1.61 (m, 1H, H21 C_8H_{11}), 1.56 (m, 1H, H17 C_8H_{12}), 1.53 (m, 1H, H12 C_8H_{12}), 1.40 (m, 1H, H22 C_8H_{11}), 1.31 (m, 1H, H10 C_8H_{12}), 1.31 (m, 1H, H12 C_8H_{12}), 1.16 (m, 1H, H14 C_8H_{12}), 1.01 (s, 3H, SiMe), 0.92 (s, 3H, SiMe), 0.10 (dddd, 1H, H21 C_8H_{11}, $^2J_{HH}$ = 17.6, $^3J_{HH}$ = 13.1, $^3J_{HH}$ = 8.9, $^3J_{HH}$ = 3.3). ^{13}C{^{1}H} NMR (125.81 MHz, C_6D_6, 301 K): 154.1 (C1 $C_9H_{19}N_3Si$, quaternary), 137.85 (C25 C_8H_{11}), 123.13 (C24 C_8H_{11}), 105.38 (C19 C_8H_{11}), 72.38 (C10 C_8H_{12}), 71.58 (C7 $C_7H_{12}N_3$), 71.12 (C18 C_8H_{11}), 66.89 (C15 C_8H_{12}), 66.07(C14 C_8H_{12}), 57.13 (C20 C_8H_{11}), 48.13 (C2 $C_7H_{12}N_3$), 47.56 (C12 C_8H_{12}), 46.51 (C4 or C5 $C_7H_{12}N_3$), 41.04 (C4 or C5 $C_7H_{12}N_3$), 37.64 (C3 or C6 $C_7H_{12}N_3$), 36.08 (C16 C_8H_{12}), 28.21 (C3 or C6 $C_7H_{12}N_3$), 26.86 (C13 C_8H_{12}), 26.42 (C25 C_8H_{11}), 25.96 (C22 C_8H_{11}), 24.78 (C11 C_8H_{12}), 23.65 (C21 C_8H_{11}), 23.42 (C17 C_8H_{12}), 6.43 (SiMe), 2.38 (SiMe). (^{29}Si,^{1}H)-HMQC NMR (C_6D_6, 99.40 MHz, 301 K): 71.70. Anal. Calcd for $C_{25}H_{41}N_3SiRu$: C, 58.56; H, 8.06; N, 8.20. Found: C, 58.39; H, 8.33; N, 8.19.

*Synthesis of [Ru(H){κ-Si,N-(SiMe$_2$)($C_7H_{12}N_3$)}$_3$] (**3a**).* A THF solution (1 mL) of 1,5,7-triazabicyclo[4.4.0]dec-6-ene-*N*-dimethylsilazane (0.169 g, 0.858 mmol) was added to a THF solution (6 mL) of [Ru{κ-Si,N-(SiMe$_2$)($C_7H_{12}N_3$)}(η^4-C_8H_{12})((η^3-C_8H_{11})] (0.200 g, 0.390 mmol). The resulting orange solution was stirred for 3.5 h at 60 °C. After cooling to room temperature, the solvent was evaporated to leave a dark orange solid that was dried under vacuum for 1 h, washed with cold pentane (3 × 3 mL, −5 °C), and dried under vacuum for a further 1 h to afford the pure product, an orange powder (0.108 g, 40%). Crystals suitable for X-ray analysis were grown from slow diffusion of pentane into a saturated THF solution. ^{1}H NMR (500.33 MHz, C_6D_6, 301 K): (see **1a** in Chart 1 for ligand atom numeration) 3.51 (ddd, 3H, H2 $C_7H_{12}N_3$, $^2J_{HH}$ = −13.2, $^3J_{HH}$ = 8.1, $^4J_{HH}$ = 3.9), 3.34 (m, 3H, H2 $C_7H_{12}N_3$), 3.30 (m, 3H, H7 $C_7H_{12}N_3$), 3.20 (m, 3H, H7 $C_7H_{12}N_3$), 2.93 (m, 3H, H4 $C_7H_{12}N_3$), 2.86 (ddd, 3H, H4 $C_7H_{12}N_3$, $^2J_{HH}$ = −16.2, $^3J_{HH}$ = 10.8, $^4J_{HH}$ = 5.5), 2.74 (ddd, 6H, H5 $C_7H_{12}N_3$, $^2J_{HH}$ = −17.1, $^3J_{HH}$ = 10.8, $^4J_{HH}$ = 6.2), 1.80 (m, 6H, H3 $C_7H_{12}N_3$), 1.64 (m, 3H, H6 $C_7H_{12}N_3$), 1.58 (m, 3H, H6 $C_7H_{12}N_3$), 0.84 (s, 9H, SiMe), 0.60 (s, 9H, SiMe), −15.83 (s, 1H, Ru−H, J_{SiHapp} = 9.0). ^{13}C{^{1}H} NMR (125.80 MHz, C_6D_6, 301 K): 156.05 (C1, $C_7H_{12}N_3$), 48.88 (C5, $C_7H_{12}N_3$), 48.83 (C4, $C_7H_{12}N_3$), 44.81 (C2, $C_7H_{12}N_3$), 40.96 (C7, $C_7H_{12}N_3$), 24.08 (C3, $C_7H_{12}N_3$), 24.00 (C6, $C_7H_{12}N_3$), 9.18 (SiMe), 4.71(SiMe).^{29}Si ^{1}H DEPT NMR (THF-d_8, 99.40 MHz, 298 K): 56.98. ^{29}Si {^{1}H} DEPT NMR (THF-d_8, 99.40 MHz, 193 K): 56.24. Anal. Calcd for $C_{27}H_{55}N_9Si_3Ru$·0.3THF (C_4H_8O): C, 47.52; H, 8.12; N, 18.24. Found: C, 47.64; H, 8.01; N, 18.06. The amount of incorporated THF was determined from NMR integration.

*Synthesis of [Ru(H)(η^2-H−SiMe$_2$)κ-N-($C_7H_{12}N_3$){κ-Si,N-(SiMe$_2$)-($C_7H_{12}N_3$)}$_2$]$^+$[PF$_6$]$^-$ (**4aPF$_6$**).* A CH_2Cl_2 solution (3 mL) of **3a** (0.150 g, 0.217 mmol) was added to a CH_2Cl_2 solution (3 mL) of [NH$_4$]$^+$[PF$_6$]$^-$ (0.044 g, 0.270 mmol). The resulting pink solution with a white suspended solid was stirred for 4 h at 25 °C to give a homogeneous orange solution. The solution was filtered through Celite, and the solvent was evaporated to afford the pure product, an orange solid (0.120 g, 66%). Yellow crystals suitable for X-ray diffraction were grown from slow diffusion of a saturated THF solution into a layer of pentane at room temperature. ^{1}H NMR (400.13 MHz, CD_2Cl_2, 298 K): 3.22 (m, 18H, $C_7H_{12}N_3$), 2.99 (m, 3H, $C_7H_{12}N_3$), 2.92 (m, 3H, $C_7H_{12}N_3$), 1.92−1.77 (m, 8H, $C_7H_{12}N_3$), 0.37 (s, 9H, SiMe), 0.31 (s, 9H, SiMe), −15.71 (s, 2H, Ru−H, J_{SiHapp} = 17). ^{1}H NMR (500.32 MHz, THF-d_8, 193 K): no decoalescence, −16.81 (s, 2 H, J_{SiHapp} = 17). $t_{1\ min}$ of the hydride signal in THF-d_8 at 500.32 MHz and 223 K is 500 ms. ^{13}C {^{1}H} NMR (100.62 MHz, CD_2Cl_2, 298 K): 156.52 (s, quaternary), 48.60 (s, $C_7H_{12}N_3$), 48.35 (s, $C_7H_{12}N_3$), 44.27 (s, $C_7H_{12}N_3$), 41.07 (s, $C_7H_{12}N_3$), 23.09 (s, $C_7H_{12}N_3$), 22.99 (s, $C_7H_{12}N_3$), 8.07 (s, SiMe), 3.48 (s, SiMe). ^{31}P {^{1}H} NMR (161.96 MHz, CD_2Cl_2, 298 K): −144.51 (sept, PF_6, $^1J_{PF}$ = 711). (^{29}Si,^{1}H)-HMQC GP QF NMR (79.50 MHz, CD_2Cl_2, 298 K): 45.7. ^{29}Si HMQC GP QF NMR (99.40 MHz, THF-d_8, 193 K): 46.0. IR Nujol (cm^{-1}) 2111, 2042 (weak). Anal. Calcd for $C_{27}H_{56}F_6N_9PRuSi_3$: C, 38.74; H, 6.74; N, 15.06. Found: C, 38.45; H, 6.80; N, 14.75.

X-ray and Neutron Structural Analysis. The crystal structures of **2a**, **2b**, **2c**, **3a**, **3b pent**, **3b hex**, **3c**, **4aPF$_6$**, and **4aBAr$^F_4$** were determined by X-ray diffraction. Data were collected at low temperature (173 K for **3b hex** and 100 K for the other compounds) using graphite monochromated Mo Kα radiation (λ = 0.71073 Å). The structures were solved by direct methods and refined by least-squares on F^2 using anisotropic displacement parameters for the non-hydrogen atoms. Hydrogen atoms were placed in calculated positions and refined using a riding model; the hydrides were located by difference

dx.doi.org/10.1021/ic4027199 | Inorg. Chem. 2014, 53, 1156−1165

Fourier maps and refined isotropically. Selected crystallographic and refinement data are listed in Table 6 , and more details on the data collections and refinements are given in the Supporting Information.

Neutron Data for 3a. $C_{27}H_{55}N_9RuSi_3$, M_w= 691.11, monoclinic, space group $P2_1/c$. a = 9.3703(2) Å, b = 18.4278(5) Å, c = 18.8875(5) Å, β = 92.530(1)°, V = 3258.2 (1)Å^3, Z = 4, λ = 1.1709(1) Å. A prismatic crystal (volume ca. 19 mm^3) was sealed, under Ar, inside a thin-walled quartz tube. The sample was mounted on a Displex cryorefrigerator on the ILL D19 diffractometer equipped with a horizontally curved banana-shaped position-sensitive detector and cooled to 20 K. A total of 31 238 Bragg reflections were collected ($4.9 < \theta < 60.3$), of which 9863 were unique. The Bragg intensities were corrected for attenuation by the vanadium Displex heat shields and analytically for the crystal absorption. The starting structural model was based on the atomic coordinates from the X-ray structure, and the position of the hydride was found from a difference Fourier map. The structure was refined by full matrix least-squares using anisotropic displacement parameters for all atoms. Final R_1 = 0.0439 and wR_2 = 0.1042 for 9100 observed reflections [$I > 2\sigma(I)$] and 856 parameters. More details of the data collection and refinement are given in the Supporting Information.

■ ASSOCIATED CONTENT

Supporting Information

Solid-state NMR data. X-ray structural data. Neutron data details for complex **3a**. CIF files for complexes **2**−**4** (X-ray and neutron). Synthetic procedures for **2b**, **2c**, **3b**, **3c**, and **4aBAr$^F_4$** and deprotonation of **4aPF$_6$**. Computational details. This material is available free of charge via the Internet at http://pubs.acs.org. Cambridge Crystallographic Data Centre deposition numbers: **2a**, CCDC 947551; **2b**, CCDC 947552; **2c**, CCDC 947553; **3a,** CCDC 947554 and CCDC 947558 (neutron data); **3b,** CCDC 947555; **3c pent**, CCDC 947556; **3b hex**, CCDC 947557; **4aPF$_6$** CCDC 947559; and **4aBAr$^F_4$** CCDC 947560.

■ AUTHOR INFORMATION

Corresponding Authors

*E-mail: mary.grellier@lcc-toulouse.fr(M.G.).
*E-mail: sylviane.sabo@lcc-toulouse.fr (S.S.-E.).

Author Contributions

The manuscript was written through contributions of all authors. All authors have given approval to the final version of the manuscript.

Notes

The authors declare no competing financial interest.

■ ACKNOWLEDGMENTS

We thank the CNRS and CONACYT for support and Johnson Matthey Plc for the generous gift of hydrated ruthenium trichloride. K.A.S. thanks the French Ministry of Research for a Ph.D. fellowship. Computer time was given by the HPC resources of CALMIP (Toulouse, France) under the allocation 2012-[P0909]. A.A. thanks MIUR (PRIN 2009) for financial support.

■ REFERENCES

(1) (a) Corey, J. Y.; Braddock-Wilking, J. *Chem. Rev.* **1999**, *99*, 175−292. (b) Corey, J. Y. *Chem. Rev.* **2011**, *111*, 863−1071. (c) Kubas, G. J. *Chem. Rev.* **2007**, *107*, 4152−4205. (d) Kubas, G. J. *Metal Dihydrogen and σ-Bond Complexes: Structure, Theory, and Reactivity*; Kluwer Academic/Plenum Publishers: New York, 2001. (e) Alcaraz, G.; Sabo-Etienne, S. *Coord. Chem. Rev.* **2008**, *252*, 2395−2409. (f) Perutz, R. N.; Sabo-Etienne, S. *Angew. Chem., Int. Ed.* **2007**, *46*, 2578−2592. (g) Ulrich, S. *Adv. Organomet. Chem.* **1990**, *30*, 151−187.

(2) Lachaize, S.; Sabo-Etienne, S. *Eur. J. Inorg. Chem.* **2006**, 2115−2127.

(3) (a) Nikonov, G. I. *Adv. Organomet. Chem.* **2005**, *53*, 217−309. (b) Ignatov, S. K.; Rees, N. H.; Tyrrell, B. R.; Dubberley, S. R.; Razuvaev, A. G.; Mountford, P.; Nikonov, G. I. *Chem.—Eur. J.* **2004**, *10*, 4991−4999. (c) Nikonov, G. I.; Kuzmina, L. G.; Howard, J. A. K. *J. Chem. Soc., Dalton Trans.* **2002**, 3037−3046. (d) Nikonov, G. I. *Angew. Chem., Int. Ed.* **2001**, *40*, 3353−3355.

(4) (a) Scherer, W.; Eickerling, G.; Tafipolsky, M.; McGrady, G. S.; Sirsch, P.; Chatterton, N. P. *Chem. Commun.* **2006**, 2986−2988. (b) McGrady, G. S.; Sirsch, P.; Chatterton, N. P.; Ostermann, A.; Gatti, C.; Altmannshofer, S.; Herz, V.; Eickerling, G.; Scherer, W. *Inorg. Chem.* **2009**, *48*, 1588−1598. (c) Scherer, W.; Meixner, P.; Barquera-Lozada, J. E.; Hauf, C.; Obenhuber, A.; Bruck, A.; Wolstenholme, D. J.; Ruhland, K.; Leusser, D.; Stalke, D. *Angew. Chem., Int. Ed.* **2013**, *52*, 6092−6096.

(5) Atheaux, I.; Delpech, F.; Donnadieu, B.; Sabo-Etienne, S.; Chaudret, B.; Hussein, K.; Barthelat, J.-C.; Braun, T.; Duckett, S. B.; Perutz, R. N. *Organometallics* **2002**, *21*, 5347−5357.

(6) (a) Trost, B. M.; Ball, Z. T. *J. Am. Chem. Soc.* **2002**, *125*, 30−31. (b) Seyferth, D.; Stewart, R. M. *Appl. Organomet. Chem.* **1997**, *11*, 813−832.

(7) Koenigs, C. D. F.; Mueller, M. F.; Aiguabella, N.; Klare, H. F. T.; Oestreich, M. *Chem. Commun.* **2013**, *49*, 1506−1508.

(8) Deschner, T.; Tornroos, K. W.; Anwander, R. *Inorg. Chem.* **2011**, *50*, 7217−7228.

(9) Ayed, T.; Barthelat, J.-C.; Tangour, B.; Pradère, C.; Donnadieu, B.; Grellier, M.; Sabo-Etienne, S. *Organometallics* **2005**, *24*, 3824−3826.

(10) Gath, J.; Hoaston, G. L.; Vold, R. L.; Berthoud, R.; Coperet, C.; Grellier, M.; Sabo-Etienne, S.; Lesage, A.; Emsley, L. *Phys. Chem. Chem. Phys.* **2009**, *11*, 6962−6971.

(11) Grellier, M.; Ayed, T.; Barthelat, J.-C.; Albinati, A.; Mason, S.; Vendier, L.; Coppel, Y.; Sabo-Etienne, S. *J. Am. Chem. Soc.* **2009**, *131*, 7633−7640.

(12) Smart, K. A.; Grellier, M.; Vendier, L.; Mason, S. A.; Capelli, S. C.; Albinati, A.; Sabo-Etienne, S. *Inorg. Chem.* **2013**, *52*, 2654−2661.

(13) Wiseman, G. H.; Wheeler, D. R.; Seyferth, D. *Organometallics* **1986**, *5*, 146−152.

(14) (a) Shimada, S.; Rao, M. L. N.; Hayashi, T.; Tanaka, M. *Angew. Chem., Int. Ed.* **2001**, *40*, 213−216. (b) Angelini, A.; Aresta, M.; Dibenedetto, A.; Pastore, C.; Quaranta, E.; Chierotti, M. R.; Gobetto, R.; Papai, I.; Graiff, C.; Tiripicchio, A. *Dalton Trans.* **2009**, 7924−7933. (c) *Solid-State NMR Spectroscopy: Principles and Applications*; Duer, M. J., Ed.; Blackwell Science Ltd: Oxford, 2002. (d) Walaszek, B.; Adamczyk, A.; Pery, T.; Yeping, X.; Gutmann, T.; Amadeu, N. d. S.; Ulrich, S.; Breitzke, H.; Vieth, H. M.; Sabo-Etienne, S.; Chaudret, B.; Limbach, H.-H.; Buntkowsky, G. *J. Am. Chem. Soc.* **2008**, *130*, 17502−17508. (e) Chierotti, M. R.; Gobetto, R. *Eur. J. Inorg. Chem.* **2009**, 2581−2597. (f) Thibault, M.-H.; Lucier, B. E. G.; Schurko, R. W.; Fontaine, F.-G. *Dalton Trans.* **2009**, 7701−7716. (g) Rossini, A. J.; Mills, R. W.; Briscoe, G. A.; Norton, E. L.; Geier, S. J.; Hung, I.; Zheng, S.; Autschbach, J.; Schurko, R. W. *J. Am. Chem. Soc.* **2009**, *131*, 3317−3330. (h) Lucier, B. E. G.; Tang, J. A.; Schurko, R. W.; Bowmaker, G. A.; Healy, P. C.; Hanna, J. V. *J. Phys. Chem. C* **2010**, *114*, 7949−7962. (i) Kapdi, A. R.; Whitwood, A. C.; Williamson, D. C.; Lynam, J. M.; Burns, M. J.; Williams, T. J.; Reay, A. J.; Holmes, J.; Fairlamb, I. J. S. *J. Am. Chem. Soc.* **2013**, *135*, 8388−8399. (j) Johnston, K. E.; O'Keefe, C. A.; Gauvin, R. M.; Trebosc, J.; Delevoye, L.; Amoureux, J.-P.; Popoff, N.; Taoufik, M.; Oudatchin, K.; Schurko, R. W. *Chem.—Eur. J.* **2013**, *19*, 12396−12414. (k) Zou, F.; Furno, F.; Fox, T.; Schmalle, H. W.; Berke, H.; Eckert, J.; Chowdhury, Z.; Burger, P. *J. Am. Chem. Soc.* **2007**, *129*, 7195−7205.

(15) Gloaguen, Y.; Alcaraz, G.; Petit, A. S.; Clot, E.; Coppel, Y.; Vendier, L.; Sabo-Etienne, S. *J. Am. Chem. Soc.* **2011**, *133*, 17232−17238.

(16) (a) Watanabe, T.; Hashimoto, H.; Tobita, H. *Chem.—Asian J.* **2012**, *7*, 1408−1416. (b) Mork, B. V.; Tilley, T. D.; Schultz, A. J.; Cowan, J. A. *J. Am. Chem. Soc.* **2004**, *126*, 10428−10440.

(c) Bakhmutov, V. I.; Howard, J. A. K.; Keen, D. A.; Kuzmina, L. G.; Leech, M. A.; Nikonov, G. I.; Vorontsov, E. V.; Wilson, C. C. *J. Chem. Soc., Dalton Trans.* **2000**, 1631−1635. (d) Tanaka, I.; Ohhara, T.; Niimura, N.; Ohashi, Y.; Jiang, Q.; Berry, D. H.; Bau, R. *J. Chem. Res., Synop.* **1999**, *14*−*15*, 180−192. (e) Schubert, U.; Ackermann, K.; Woerle, B. *J. Am. Chem. Soc.* **1982**, *104*, 7378−7380.
(17) Pertici, P.; Vitulli, G.; Paci, M.; Porri, L. *J. Chem. Soc., Dalton Trans.* **1980**, 1961−1964.
(18) Vinogradov, E.; Madhu, P. K.; Vega, S. *Chem. Phys. Lett.* **2002**, *354*, 193−202.
(19) van Rossum, B. J.; Förster, H.; de Groot, H. J. M. *J. Magn. Reson.* **1997**, *124*, 516−519.

dx.doi.org/10.1021/ic4027199 | *Inorg. Chem.* 2014, 53, 1156−1165